



# Mitochondrial ROS signalling requires uninterrupted electron flow and is lost during ageing in flies

Charlotte Graham · Rhoda Stefanatos · Angeline E. H. Yek · Ruth V. Spriggs · Samantha H. Y. Loh · Alejandro Huerta Uribe · Tong Zhang · L. Miguel Martins · Oliver D. K. Maddocks · Filippo Scialo · Alberto Sanz

Received: 21 October 2021 / Accepted: 22 March 2022 / Published online: 30 March 2022  
© The Author(s) 2022

**Abstract** Mitochondrial reactive oxygen species (mtROS) are cellular messengers essential for cellular homeostasis. In response to stress, reverse electron transport (RET) through respiratory complex I generates high levels of mtROS. Suppression of ROS production via RET (ROS-RET) reduces survival

under stress, while activation of ROS-RET extends lifespan in basal conditions. Here, we demonstrate that ROS-RET signalling requires increased electron entry and uninterrupted electron flow through the electron transport chain (ETC). We find that in old fruit flies, ROS-RET is abolished when electron flux is decreased and that their mitochondria produce consistently high levels of mtROS. Finally, we demonstrate that in young flies, limiting electron exit, but not entry, from the ETC phenocopies mtROS generation observed in old individuals. Our results elucidate the mechanism by which ROS signalling is lost during ageing.

Filippo Scialo and Alberto Sanz share seniorship.

**Supplementary Information** The online version contains supplementary material available at <https://doi.org/10.1007/s11357-022-00555-x>.

C. Graham · R. Stefanatos · A. E. H. Yek  
Institute for Cell and Molecular Biosciences,  
Newcastle University Institute for Ageing, Newcastle  
University, Campus for Ageing and Vitality,  
Newcastle upon Tyne NE4 5PL, UK

R. Stefanatos  
Faculty of Medical Sciences, Wellcome Centre  
for Mitochondrial Research, Biosciences Institute,  
Newcastle University, Newcastle upon Tyne NE4 5PL, UK

R. V. Spriggs · S. H. Y. Loh · L. M. Martins  
MRC Toxicology Unit, University of Cambridge,  
Cambridge CB2 1QR, UK

R. V. Spriggs  
Hearing Sciences, School of Medicine, University  
of Nottingham, Nottingham NG7 2UH, UK

A. H. Uribe · T. Zhang · O. D. K. Maddocks  
Institute of Cancer Sciences, Wolfson Wohl  
Cancer Research Centre, University of Glasgow,  
Glasgow G61 1QH, UK

*Present Address:*

T. Zhang  
Novartis Institutes for BioMedical Research,  
Shanghai 201203, China

F. Scialo (✉) · A. Sanz (✉)  
Institute of Molecular, Cell and Systems Biology, College  
of Medical, Veterinary and Life Sciences, University  
of Glasgow, Glasgow G12 8QQ, UK  
e-mail: Filippo.Scialo@unicampania.it

A. Sanz  
e-mail: Alberto.Sanzmontero@glasgow.ac.uk

F. Scialo  
Dipartimento Di Scienze Mediche Traslazionali,  
Università Degli Studi Della Campania “Luigi Vanvitelli”,  
80131 Naples, Italy

**Keywords** Ageing · Complex I · Complex IV · *Drosophila* · Mitochondria · Reverse electron transport · Reactive oxygen species

### Abbreviations

H <sub>2</sub> O <sub>2</sub>	Hydrogen peroxide
CI	Complex I
CII	Complex II
CIII	Complex III
CIV	Complex IV
CoQ	Coenzyme Q
CYA	Cyanide
ETC	Electron transport chain
PPP	Pentose phosphate pathway
pmf	Proton motive force
RET	Reverse electron transport
mtROS	Mitochondrial reactive oxygen species
ROS-RET	ROS produced via reverse electron transport
ROT	Rotenone
TCA,	Tricarboxylic acid
TS	Thermal stress

### Introduction

Mitochondria are double-membrane organelles which produce a significant amount of cellular energy. Mitochondria are also instrumental for the synthesis of iron-sulphur clusters, nucleotides for DNA replication and the generation of metabolic intermediates required for anabolism [45]. These fundamental roles mean that mitochondrial function influences crucial processes affecting cell growth, differentiation and death by controlling senescence and apoptosis [8, 18]. A hallmark of ageing is the accumulation of damaged mitochondria that produce high levels of mitochondrial reactive oxygen species (mtROS) [19]. The negative consequences of elevated levels of ROS, i.e. loss of redox signalling and oxidative stress, are well known [43], however, it is unclear how and why this occurs. Due to the central role of mitochondria in maintaining cellular homeostasis, we anticipate that inhibition of “mitochondrial ageing” will improve healthspan and contribute to a delayed onset of diseases associated with ageing.

To understand how mitochondrial ageing occurs, we must identify the physiological processes regulated by mtROS and study how they are altered during ageing. It is therefore imperative that the connection between changes in mtROS and the accumulation of respiratory-deficient mitochondria is understood. In the past, we have shown that in response to stress, fly mitochondria produce ROS via reverse electron transport (RET) (ROS-RET) [41]. ROS-RET occurs under particular conditions, when both a highly reduced coenzyme Q (CoQ) pool and elevated proton motive force (pmf) coincide to allow RET from ubiquinol to CI [33]. Suppression of ROS-RET under stress prevents an adaptative transcriptional response and shortens survival in both fruit flies [41] and mice [9]. On the other hand, stimulation of ROS-RET in basal conditions, through expression of an alternative NADH dehydrogenase, extends the lifespan of *Drosophila* [40, 40]. This indicates the existence of a mitochondrial redox signalling pathway that acts to regulate lifespan under both basal and stress conditions.

Stress adaptation in flies relies upon ROS-RET, which requires perfectly coupled mitochondria. We hypothesised that ROS-RET signalling would be affected by age-associated mitochondrial alterations, limiting stress adaptation in old individuals. Here, we resolve the mechanism mediating ROS-RET signalling in detail. We combine high-resolution respirometry and metabolomic profiling to characterise how ROS-RET occurs in vivo. We show that ROS-RET is triggered by an increase in electron entry into the electron transport chain (ETC). Next, we demonstrate that ROS-RET signalling is lost during ageing and replaced by sustained high levels of ROS production. At the organismal level, we show that loss of ROS-RET compromises stress adaptation in old individuals. Finally, we dissect the ETC alterations responsible for the loss of ROS-RET during ageing. We find that reducing electron exit in young individuals suppresses ROS-RET signalling resulting in an acute increase in ROS production upstream of complex IV (CIV). Like in old mitochondria, mitochondria where CIV is depleted are unresponsive to stress stimuli and phenocopy the mitochondrial ageing phenotype observed in aged individuals.

## Material and methods

### Fly husbandry

Wild-type flies (white Dahomey, wDAH), RNA interference (RNAi) and GAL4 driver lines were collected and cultured as in [41]. Briefly, flies were maintained on standard media (1% *Drosophila* agar type II (Dutscher Scientific, #789,150), 1.5% sucrose (Sigma, #S27480), 3% glucose (Sigma, #16,325), 3.5% dried yeast (Dutscher Scientific, #789,093), 1.5% maize (TRS), 1% wheat (MP Biomedicals, #0,290,328,805), 1% soy (Santa Cruz Biotechnology, #Sc-215897A), 3% treacle (Bidvest, #90028S), 0.5% propionic acid (VWR, #8.00605.2500), 0.1% Nipagin (Sigma, #H5501)), collected using CO<sub>2</sub> anaesthesia within 24 h of eclosion and maintained at a density of 20 flies per vial at 25 °C. Female flies 2–5 days old, unless otherwise stated, were used for all experiments. UAS-*levy*-RNAi (CG17280, 101,523) and UAS-*ND-75*-RNAi (CG2286, 100,733) were obtained from the Vienna *Drosophila* Resource Centre (VDRC), while daughterless-GAL4 (daGAL4) was acquired from the Bloomington *Drosophila* Stock Centre (BDSC). ETC inhibitors, rotenone (Santa Cruz Biotechnology, #Sc-203242) and cyanide (Sigma, #60,178), were dissolved in ethanol and water and added to the fly food at a final concentration of 600 µM and 18 mM, respectively.

### Thermal stress and lifespan studies

Thermal stress (TS) was induced by transferring flies cultured at 25 to 32 °C for 3–4 h. Except for lifespan experiments, flies were used immediately after TS for all experiments. For lifespan experiments, flies were TS three times per week for 4 h in either the presence or absence of rotenone and then returned to 25 °C (in the absence of rotenone).

### Measurement of ROS levels in *Drosophila* brains

ROS were measured in individual fly brains as described in [41]. Briefly, 2',7'-dichlorofluorescein (H<sub>2</sub>DCF) was used to detect total levels of ROS. Brains were dissected in phosphate-buffered saline (PBS). Following dissection, brains were incubated in 30 µM

H<sub>2</sub>DCF for 10 min, washed three times with 1X PBS, and imaged immediately. Images were acquired using a LSM510 confocal microscope (Zeiss) equipped with a 10×0.3 NA objective as z stacks throughout the sample, using a 488-nm line of an Argon laser to excite H<sub>2</sub>DCF. The total average fluorescence intensity of each brain was quantified using ImageJ.

### Measurement of mitochondrial oxygen consumption

Mitochondrial oxygen consumption was assessed via high-resolution respirometry using an Oxygraph 2-K (Oroboros Instruments) as described in [40, 40]. Briefly, whole flies (10–20) or fly heads (20–30) were homogenised in isolation buffer (250 mM sucrose, 5 mM Tris-HCl, 2 mM EGTA, pH 7.4). Homogenates were diluted 20 times in assay buffer (120 mM KCl, 5 mM KH<sub>2</sub>PO<sub>4</sub>, 3 mM HEPES, 1 mM EGTA, 0.5 mM MgCl<sub>2</sub>, 0.2% (w.v.) BSA, pH 7.2) for analysis. Mitochondrial activity was initiated through the addition of pyruvate (5 mM) and proline (5 mM) followed by ADP (1 mM) to initiate state 3. Oxygen consumption was quantified using Oroboros DatLab 5.0 software with oxygen flux raw values normalised to the amount of fly protein. Final values were expressed as picomoles of oxygen per min<sup>-1</sup> per mg<sup>-1</sup>.

### Metabolomic analysis by liquid chromatography-mass spectrometry (LC-MS)

In total, 20 heads per sample (three independent samples) were homogenised in ice-cold lysis solvent (methanol 50%, HPLC grade acetonitrile 30%, water 20%) and centrifuged at 13,000–15,000 rpm for 15 min at 4 °C. The supernatant was stored at –80 °C. Before analysis, samples were transferred to LC-MS vials. LC-MS measurements and related data analysis were performed as described previously [20], using a ZIC-pHILIC analytical column. LC-MS raw data were converted into mzML files using ProteoWizard. MZMine 2.10 was used for peak extraction and sample alignment. For global metabolomics, metabolites were analysed with the help of MetaboAnalyst [46]. A CSV file containing the intensity values of the peaks of all the metabolites detected was uploaded into MetaboAnalyst, and the statistical analysis tool was selected. Data were analysed with the following options: data filtering (none), data transformation (log), and data scaling (auto). Samples grouped by

treatment were analysed by ANOVA, and data were ranked according to FDR values ( $p < 0.05$ ). Afterwards, selected metabolites were used for enrichment (input type: KEEG ID/metabolites, feature type: KEEG) and pathway analysis (visualisation method: scatter plot, enrichment method: hypergeometric test; topology analysis: relative-betweenness centrality; reference metabolome: Homo sapiens KEEG) using the enrichment and pathways analysis tools of MetaBoAnalyst respectively with a cut-off of  $p \leq 0.05$ .

#### Next-generation sequencing: data acquisition and analysis

RNA was extracted from fly heads (20 heads per sample, five independent samples per condition). Heads were homogenised in TRI Reagent (Sigma) following the manufacturer's instructions. RNA was treated with DNase I (Thermo Fisher Scientific) at 37 °C for 60 min and precipitated overnight with 3 M sodium acetate and 95% ethanol. After centrifugation, pellets were dissolved in 50 µl of DNase/RNase free water. The RNA quality was confirmed using an Agilent 2100 Bioanalyzer (Agilent Technologies). Detailed experimental protocols and raw data are deposited in ArrayExpress under accession E-MTAB-7952. Briefly, next-generation sequencing data acquisition was performed using the TruSeq Stranded mRNA kit (Illumina) following the manufacturer's instructions. Raw data were acquired using an Illumina sequencer (NextSeq500) and processed using Partek Flow (Partek Inc. Missouri, USA). RNA reads were normalised using the default method (total count, add 0.0001) and aligned to Reference Index BDGP6 using STAR 2.4.d. To select transcripts that were up- or downregulated for subsequent analysis, we filtered transcripts whose fold change (FC) expression was above or below  $\pm 1.5$ , respectively, discarding those whose FDR was above 5%.

#### Statistical analysis

Data are shown as mean  $\pm$  SEM and were analysed using GraphPad Prism 9 with either unpaired student's *t* test or one-way ANOVA, with Dunnett's post-test where appropriate. In addition, lifespan data were analysed using the Kaplan–Meier log-rank test. Cartoons and schematic diagrams were generated with the help of biorender.com.

## Results

ROS-RET is activated by increased electron flow into the ETC

We and others have shown that ROS-RET requires both an increase in the redox state of the CoQ pool and a sufficiently high pmf to occur [33, 40, 39, 41]. It remains unclear, however, how these conditions would coincide in a physiologically relevant context. In mitochondria, the nature of the substrate that is oxidised (e.g. pyruvate versus fatty acids) determines where and how mtROS are generated [3, 12]. For example, increased oxidation of substrates downstream of CI, such as succinate, fatty acids, or dimethylglycine, stimulates ROS-RET [6, 12, 22]. While alterations in ROS levels reprogramme cellular metabolism [37], physiological examples of this include cellular differentiation [44] and adaptation to thermal [41] or oxidative stress [17]. Here, we dissect both the mechanism(s) that drive ROS-RET production and the downstream metabolic signals triggered by ROS-RET under TS. This type of natural stress has strong effects on reproduction and survival in insects such as fruit flies and is therefore highly relevant.

We have previously shown that 3 h of TS induces ROS-RET production in the fly brain. To further understand how ROS-RET occurs, we TS flies and measured mitochondrial oxygen consumption. We found a significant increase in state 4 (non-phosphorylating) and state 3 (phosphorylating) respiration (Fig. 1A), indicative of increased electron flow through the ETC. We believe that this increase in electron entry into the ETC is instrumental for ROS-RET production. In line with this, we have shown that reducing electron flow by depleting either CI or complex II (CII), using RNAi interference, abolishes ROS-RET in flies [41]. Similarly, depletion of CI, by knocking-out *Ndufs2*, specifically in cells of the carotid body prevents generation of ROS-RET and the adaptive response to hypoxemia in mice [10], whereas inhibition of electron flow through CI or CII, using rotenone or malonate, respectively, in mouse hearts diminished damage resulting from ischemia–reperfusion [6]. This suggests that the role of CI and CII in initiating ROS-RET production is conserved across evolution.

Next, we performed unbiased metabolomic profiling on heads from flies TS (Fig. S1A). We also

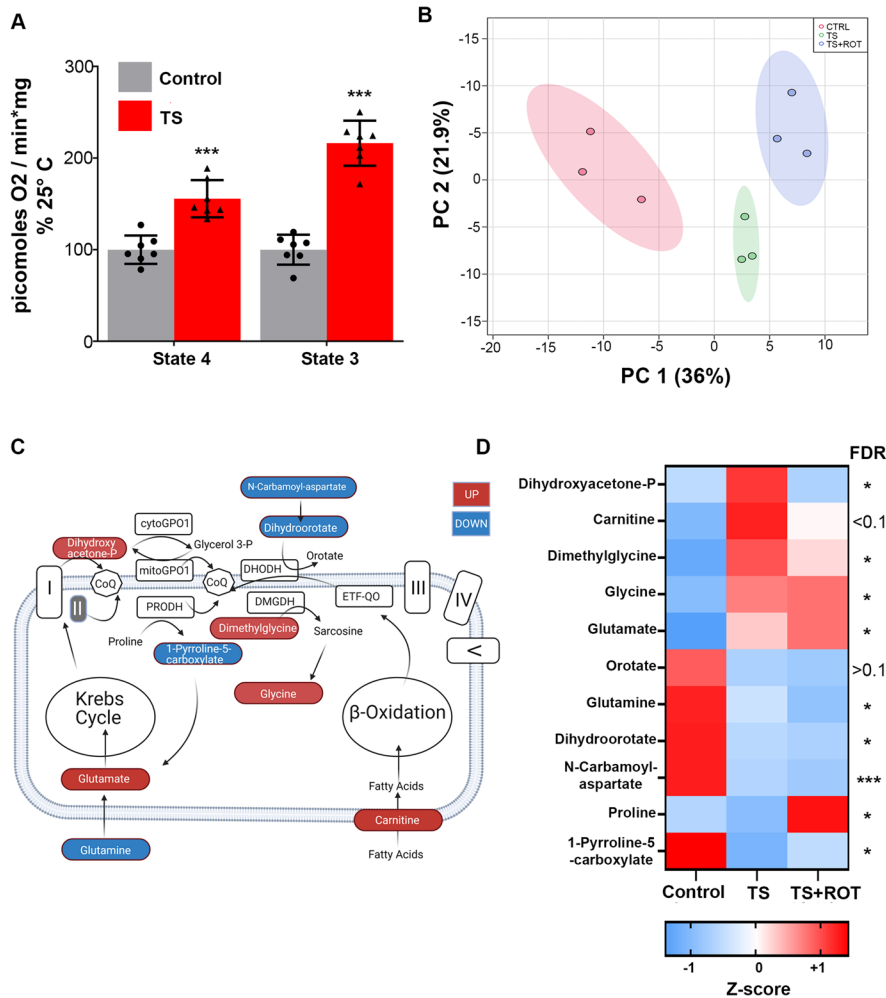


**Fig. 1** Thermal stress (TS) increases electron flow through and downstream of CI. **A** Mitochondrial oxygen consumption measured in state 4 (without ADP) and state 3 (with ADP). Data are shown as mean ± SEM. *N* = 7 per experimental group. **B** PCA analysis of the brain metabolome of Control flies and TS flies with (TS+ROT) and without rotenone (TS). **C** Schematic representation highlighting key metabolites which show alterations in response to ROS-RET and their contribution to the reduction of ubiquinone to ubiquinol. Blue colouring indicates metabolites with decreased levels, while red indicates

those with increased levels. cytoGPO1 = cytosolic glycerol-3-phosphate dehydrogenase; mtGPO1, mitochondrial glycerol-3-phosphate dehydrogenase; PRODHD, proline dehydrogenase; DHODH, dihydroorotate dehydrogenase; DMGDH, dimethylglycine dehydrogenase; ETF-QO, electron-transferring-flavo-protein dehydrogenase. **D** Heat map of metabolites potentially contributing to the generation of ROS-RET in response to TS. NS, not significant, \**p* < 0.05, \*\**p* < 0.01, \*\*\**p* < 0.001. *N* = 3 in all experiments unless otherwise stated

profiled flies fed with rotenone to distinguish between metabolic changes triggered by ROS-RET production and those as a response to heat. Rotenone blocks RET from ubiquinol to CI and is considered the gold standard for demonstrating the occurrence of ROS-RET [6, 3, 28, 39, 40]. Unsupervised principal component analysis clearly separated the three experimental groups (Fig. 1B), suggesting that specific metabolic

changes occur upstream and downstream of ROS-RET production, with potential implications for signalling and stress adaptation. We began by studying the metabolites required to trigger ROS-RET. We selected those metabolites that were significantly altered in TS flies. Pathway and enrichment analysis revealed alterations in the metabolism of amino acids such as serine and glutamate (Fig. S1B-D). This is in

line with previous observations describing that, under stress, glutamate and serine are rerouted to the ETC [48, 49] where they contribute to the reduction of ubiquinone to ubiquinol.

Manual inspection revealed significant changes in the levels of 9 metabolites with the potential to reduce ubiquinone to ubiquinol (Fig. 1C-D and S1E). Firstly, we observed a decrease in the levels of glutamine and a concomitant increase in the levels of glutamate (Fig. 1C-D and S1E). This has been described as an alternative way to feed the ETC when pyruvate oxidation is totally or partially interrupted [48]. Here, we explain the former, as an additional way to address the increase in energy demand by boosting amino acid-oxidation via the Krebs Cycle-ETC. Another way of obtaining glutamate and subsequently reductive power for the ETC via the Krebs cycle is proline oxidation [11]. Supporting the activation of this route, we detected a deep decline in the product of oxidation of proline by the mitochondrial proline dehydrogenase: 1-pyrroline-5-carboxylate (Fig. 1D and S1E). The former is further converted into glutamate by the pyrroline-5-carboxylate dehydrogenase [30]. Our interpretation of the metabolomic changes detected is further supported by data showing that insect mitochondria oxidise both proline and glycerol-3-phosphate to boost ATP production during flight [36] and when exposed to temperatures above 30 °C [15]. Accordingly, levels of dihydroxyacetone-phosphate, the product of oxidation of glycerol-3-phosphate, were increased in response to TS (Fig. 1D and Fig. S1E). It is important to note that we observed a modest increase in the levels of proline and lack of increase in the levels of dihydroxyacetone phosphate in rotenone-fed flies (Fig. 1D and S1E). We reckon that the former is to prevent NAD<sup>+</sup> depletion. Since NADH is generated from proline and glyceraldehyde 3-phosphate oxidation, to feed the ETC, and rotenone feeding prevents reoxidation of NADH (by inhibiting CI), it is plausible that in rotenone-fed flies, the oxidation of both proline and glyceraldehyde 3-phosphate is paused to prevent the catastrophic consequences of NAD<sup>+</sup> depletion. Supporting reoxidation of NADH as the problem in rotenone-fed flies, we observed a strong increase in the levels of lactate (see below for a more detailed explanation).

Secondly, we also observed evidence indicating increased oxidation of dihydroorotate, choline, and fatty acids. These three processes introduce electrons

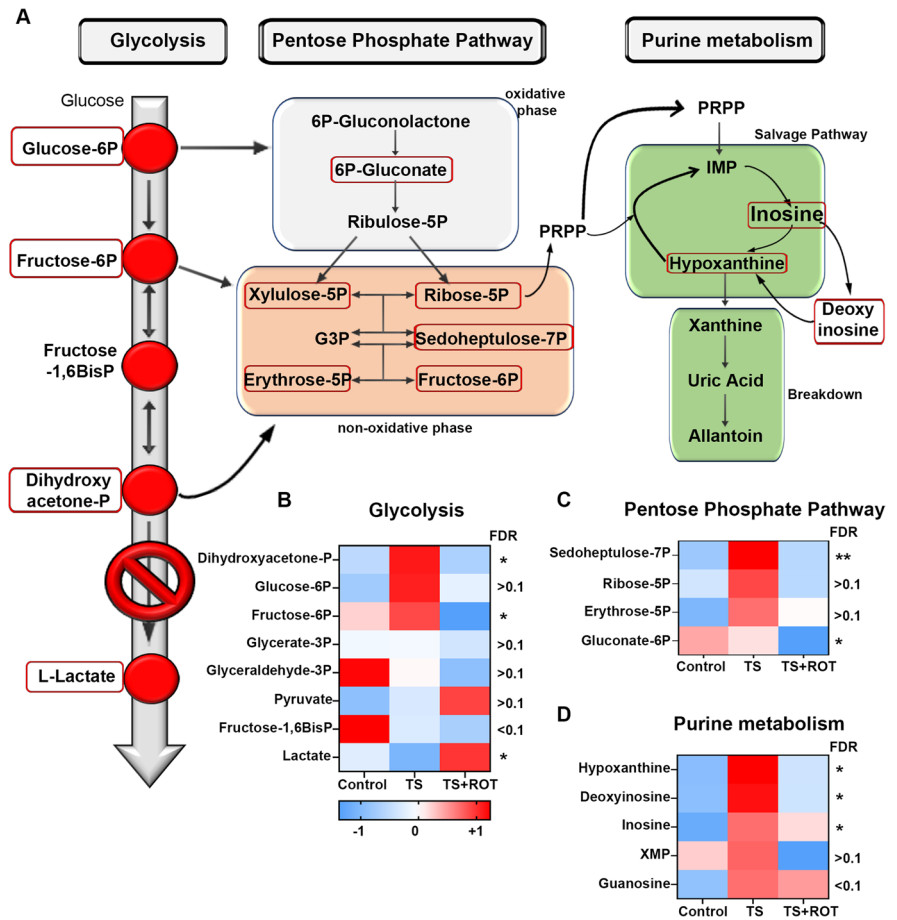
into the CoQ pool downstream of CI and CII and increased fat usage has been shown to trigger ROS-RET in mouse cells [12]. Both N-carbamoyl-aspartate and dihydroorotate levels were strongly depleted in TS flies (Fig. 1C-D and S1E). N-carbamoyl-aspartate is the precursor of dihydroorotate which is oxidised by mitochondrial dihydroorotate dehydrogenase to produce orotate, a precursor required for the synthesis of pyrimidines [23]. Supporting elevated mitochondrial oxidation of choline, we found an increase in the levels of two downstream products: dimethylglycine and glycine (Fig. 1D and S1E). Interestingly, dimethylglycine initiates ROS-RET when fed to isolated mitochondria [22]. However, the support for elevated fatty acid oxidation was modest since we only observed a small increase in the TS group that was not fed with rotenone (Fig. 1D and S1E).

All in all, our results offer indirect evidence indicating that TS activates ROS-RET production increasing mitochondrial respiration with an increased entry of electrons through both CI/II as well as other dehydrogenases. These dehydrogenases are not usually considered significant contributors to ATP production, but they have been reported to participate in ROS generation [11, 12, 22, 25].

ROS-RET reroutes glycolytic intermediates to the pentose phosphate pathway (PPP) but does not induce a short-term transcriptomic response

We next investigated the metabolic changes initiated downstream of ROS-RET by selecting metabolites that were altered (up or down) in response to TS but had their levels reverted by rotenone feeding (Fig. S1A). Enrichment and pathway analysis identified PPP, glycolysis, purine, and glutathione metabolism as the main metabolic routes modified by ROS-RET signalling (Fig. S2A-C). Our metabolomic analysis suggests that ROS-RET inhibits glycolysis, resulting in the redirection of glycolytic intermediates to PPP, allowing maintenance of NADPH levels (depleted during TS) and production of nucleotide precursors (Fig. 2B-D). Accordingly, we observed upregulation of three glycolytic intermediates (dihydroxyacetone phosphate, fructose 6-phosphate, and glucose 6-phosphate), three PPP metabolites (sedoheptulose 7-phosphate, erythrose 5-phosphate, and ribose 5-phosphate), and three components of the salvage purine synthesis pathway (hypoxanthine,

**Fig. 2** ROS-RET results in the redirection of glycolytic intermediates to the pentose phosphate pathway (PPP) to produce NADPH and nucleotide precursors. **A** Schematic representation of the biological pathways affected by ROS-RET signalling. Metabolites significantly altered by ROS are indicated in red boxes. **C–D** Heat maps of glycolytic, PPP and purine biosynthesis metabolites identified in the fly brain in control flies and TS flies with (TS+ROT) and without rotenone (TS). NS, not significant, \* $p < 0.05$ , \*\* $p < 0.01$ , \*\*\* $p < 0.001$ .  $N = 3$  in all experiments unless otherwise stated



inosine, and deoxyinosine) only in those TS flies that were not fed with rotenone (Fig. 2D and S2F).

As it can be observed in Fig. 2A, the glycolytic intermediates in TS flies are those that can be rerouted into the PPP to produce reductive and anabolic power in the form of NADPH [17]. NADPH is essential for anabolic reactions and provides reductive power to antioxidant enzymes through the reoxidation of glutathione and thioredoxin. Both functions are essential under TS, where oxidative stress is increased, and anabolic power is needed to synthesise components of the anti-stress response [13, 14]. Our results suggest that ROS-RET is required for the maintenance of NADPH levels under TS, and when ROS-RET is prevented, NADPH is quickly depleted. Accordingly, NADPH levels were below the limit of detection in the brains of TS flies in the presence of rotenone (Fig. S2D and S2F). In further support of our hypothesis, levels of gluconate 6-phosphate which is instrumental for the synthesis of NADPH

were strongly depleted only in those flies where ROS-RET was inhibited with rotenone, whereas TS flies able to produce ROS-RET maintained the concentration of gluconate 6-phosphate at the levels of controls (Fig. 2C and S2F). NADPH depletion was not caused by an increase in oxidative stress due to rotenone since the feeding of the former resulted in less mtROS production under TS as shown previously [41] and confirmed here (Fig. 3B). Correlating with low levels of mtROS, we observed an increase in the levels of reduced (GSH) and a decrease in the levels of oxidised glutathione (GSSG) (Fig. S2D and S2F) because of rotenone, further supporting a lack of oxidative stress in these flies.

PPP metabolites of the non-oxidative phase were only elevated in TS flies that were able to perform ROS-RET (Fig. 2C and S2F). Similarly, we also found that upregulation of metabolites involved in purine biosynthesis was suppressed when ROS-RET was inhibited by rotenone feeding (Fig. 2D and

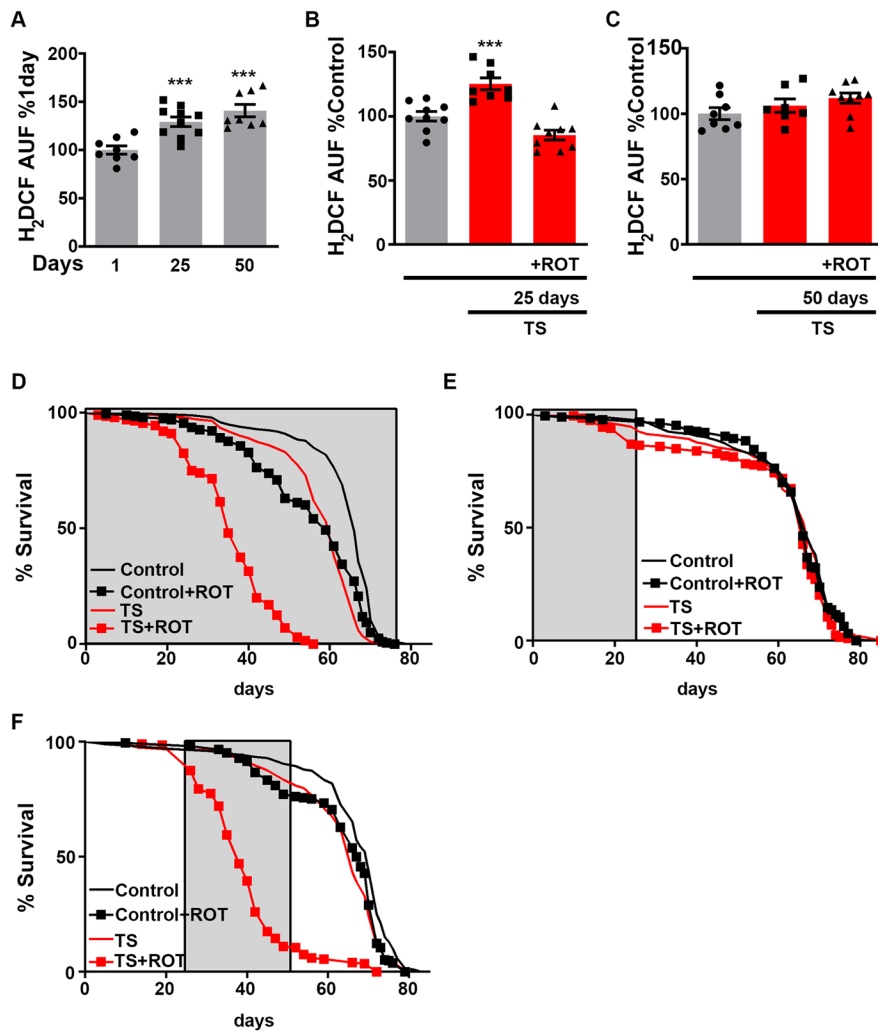


**Fig. 3** Old mitochondria continually produce high levels of ROS and are unable to activate ROS-RET signalling in response to stress. **A** ROS levels in brains of young (1 day), middle-aged (25 days) and old-aged flies (50 days).  $N=8-10$  per experimental group. **B** ROS levels in brains of middle-aged flies TS in the presence (TS+ROT) or absence of rotenone (TS).  $N=8-9$  per experimental group. **C** ROS levels in brains of old aged flies under TS in the presence of rotenone (TS+ROT) and without rotenone (TS).  $N=7-9$  per experimental group. **D** Lifespan of control flies (black line), control flies fed with rotenone 3 times a week (black squares, con-

trol+ROT), TS flies three times per week (red line, TS) and finally TS flies three times a week in the presence of rotenone (red squares, TS+ROT). Treatments were performed for the duration of fly lifespan.  $N=199-203$  per experimental group. **E** As in D, but with treatments administered only between days 1 and 25 of fly lifespan.  $N=188-204$  per experimental group. **F** Also, as in D, but with treatments administered from day 25 to Day 50.  $N=199-210$  per experimental group. **D-E** Grey shadow indicates duration of treatments. **A-C** Data are shown as mean  $\pm$  SEM. \*\*\* $p < 0.001$

S2F). Altogether, these observations suggest that ROS-RET is required for the activation of NADPH synthesis via the rerouting of glycolytic intermediates to PPP. Purines are synthesised from ribose-5-phosphate provided by the non-oxidative phase of PPP and are required for the synthesis of nucleotides

to display a long-term antistress response. In the past, we have shown that suppressing ROS-RET by expressing an alternative oxidase abolishes the transcriptional response to TS [41], and here we provide a mechanistic explanation of how this occurs at the metabolic level. Of note, we observed upregulation of



pyrimidine biosynthesis that seems to be independent of ROS-RET (see Fig. 1D and S1E and section above). A similar “glycolysis-to-PPP-purine synthesis rerouting” has been reported in glioma stem cells for adaptation to acidotic stress [47] as well as in human keratinocytes and mouse macrophages exposed to increasing concentrations of H<sub>2</sub>O<sub>2</sub> [17] or lipopolysaccharide (LPS) [4]. The LPS study is particularly relevant as increased ROS levels after LPS is a result of ROS-RET, which is suppressed in the presence of rotenone [24], as occurs under TS.

In the past, we have shown that the long-term transcriptomic response to TS requires ROS-RET signalling [41]. Here, we have analysed the brain specific transcriptome to investigate if manipulation of ROS-RET causes changes at the transcriptomic level in addition to the metabolomic level. As expected, we found upregulation of anti-stress pathways, such as the heat-shock response [42]. However, interruption of ROS-RET, via rotenone feeding did not result in any significant transcriptomic changes (Fig. S2E), and we found only one gene differentially regulated in the brains of TS flies fed with rotenone. This is like what has been described in human cells exposed to H<sub>2</sub>O<sub>2</sub> and UV radiation, where a short-term metabolomic response occurs before any transcriptional changes [17]. In summary, our results indicate that ROS-RET elicits an acute metabolic response to TS.

Ageing is characterised by consistently high levels of mtROS and the loss of ROS-RET signalling

High-resolution respirometry and metabolomic profiling showed that ROS-RET relies on increased mitochondrial oxygen consumption. Accordingly, we and others have demonstrated that interrupting electron flow by depleting subunits of CI or CII prevents ROS-RET signalling [6, 10, 40, 39, 41]. Since ageing is characterised by the decrease of mitochondrial respiration [34, 35, 40, 39], we anticipated that ROS-RET would be altered in old individuals. To test our hypothesis, we measured ROS levels in the brain of young (~1 day), middle-aged (~25 days), and old-aged flies (~50 days). We chose to study old- and middle-aged flies because mitochondrial oxygen consumption is decreased in the first group but not in the second [40, 40], and therefore if our hypothesis was correct ROS-RET should only be altered in old flies.

First, and in accordance with what we and others have reported [1, 7, 34, 35, 40, 39], we observed an accumulation of mtROS levels with age (Fig. 3A). We then decided to test the capacity to generate ROS-RET by exposing middle- and old-aged flies to TS, in the presence or absence of rotenone. In line with our hypothesis, ROS-RET production in response to TS was only detected in brains of flies with unaltered mitochondrial oxygen consumption, i.e., we detected activation of ROS-RET in middle- but not in old-aged flies (Fig. 3B and 3C). In old flies, levels of ROS did not change in response to TS and rotenone feeding did not alter the high levels of ROS, proving that they are not RET derived (Fig. 3C). Furthermore, rotenone treatment of flies in basal conditions led to increased mitochondrial ROS levels in young but not in old-aged flies (Fig. S3A, B). Our results show that during ageing CI stops producing ROS in response to both TS and rotenone and suggest that age-related loss of mitochondrial respiratory capacity [34, 35, 40, 39] results in the abolition of the activation of ROS-RET signalling in response to stress [40].

Finally, we examined the physiological relevance of ROS-RET loss. We reasoned that if ROS-RET was important for stress adaptation, then stress adaptation would be severely impacted during ageing when ROS-RET signalling is diminished. To test our hypothesis, we placed flies under TS for 4 h, three times a week, in either the presence or absence of rotenone. We performed three independent experiments where TS treatments were applied as follows: (a) for the duration of fly lifespan, (b) for the first 25 days of lifespan, or (c) from day 25 to day 50 (for details, see Fig. S3C). In experimental conditions (a), rotenone feeding dramatically shortened the lifespan of TS flies, whereas it only minimally affected the lifespan of flies in basal conditions. However, this differential effect was only evident when the flies were older than 20 days (Fig. 3D). Accordingly, when treatments (including rotenone) were stopped at day 25 (b), no differences in lifespan were observed (Fig. 3E). Conversely, when treatments began from middle age for 25 days (c), rotenone feeding severely shortened survival when flies were under TS (Fig. 3F). These results, along with the ROS measurements performed in middle- and old-aged flies, indicate that the ability to activate ROS-RET signalling progressively diminishes during ageing and that further suppression of

ROS-RET through rotenone feeding in old individuals severely compromises survival.

Blocking mitochondrial electron exit mimics the mtROS profile observed in old individuals

To complete our study, we decided to investigate which alterations in the ETC were potentially responsible for the age-related increase in ROS levels observed in mitochondria in aged brains. We hypothesised that the accumulation of mtROS might be caused by problems in electron exit from the ETC. This would cause a build-up of electrons in the ETC, increasing the likelihood of electrons reducing oxygen to superoxide directly. This has been observed in vitro in fly mitochondria exposed to the complex IV inhibitor cyanide [35] and in mouse mitochondria from COX15 knock-out mice [9]. We predicted that this mechanism also operates in vivo during ageing. To test our hypothesis, we first decreased electron entry by depleting *ND-75*, a CI subunit, (Fig. S4A). This

resulted in a ~50% decrease in mitochondrial respiration (Fig. S4B), analogous to the decrease observed in old flies [34, 35, 40, 39]. Depletion of *ND-75* did not affect ROS levels in basal conditions but prevented ROS-RET under TS (Fig. 4A–B), confirming our previous results [41]. This was not unexpected as reducing electron entry without blocking movement through the ETC does not increase electron leak.

We then suppressed electron exit via depletion of *levy*, a CIV subunit, (Fig. S4C). As with *ND-75*, knock-down of *levy* also decreased mitochondrial respiration by 50% (Fig. S4D). However, knock-down of *levy* increased ROS levels in the brain (Fig. 4C), indicating that decreased electron exit increases mtROS in the fly brain, as it has been shown to do in isolated mitochondria [9, 35]. Interestingly, no increase in mtROS was observed in response to TS in *levy* mutants (Fig. 4D, E). This failure to activate ROS-RET is precisely what occurs in old flies. Finally, we tested whether reducing CIV levels was sufficient to activate ROS-RET production by feeding flies with

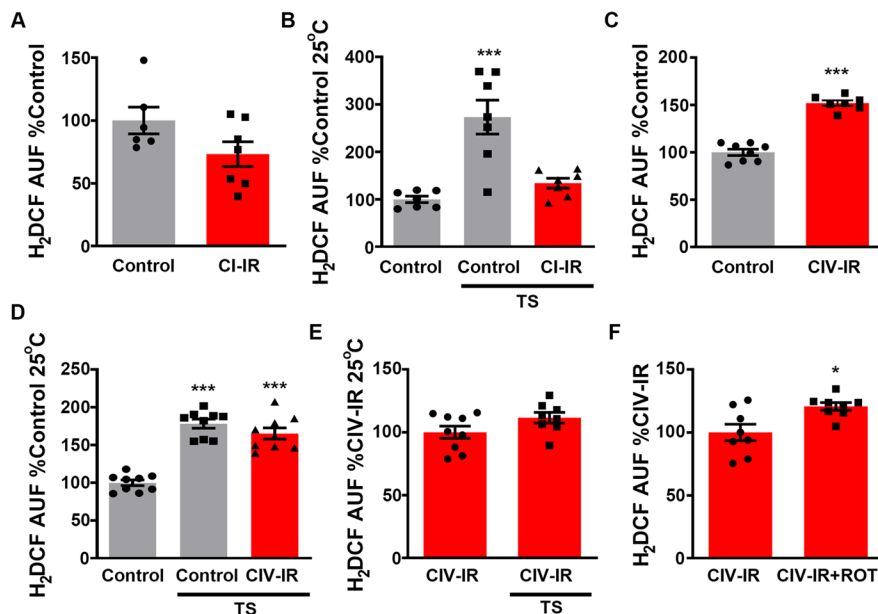


**Fig. 4** Depletion or inhibition of mitochondrial complex IV (CIV) mimics mitochondrial ROS production observed in old individuals. **A** ROS levels in brains of flies with depleted CI (CI-IR) and controls.  $N=6-7$  per experimental group. **B** ROS levels in brains of TS flies with depleted CI (CI-IR) and controls.  $N=7$  per experimental group. **C** ROS levels in brains of flies with depleted CIV (CIV-IR) and controls.  $N=7-9$  per experimental group. **D** ROS levels in brains of TS flies with

depleted CIV (CIV-IR) and controls.  $N=9$  per experimental group. **E** ROS levels in brains of flies with depleted CIV levels (CIV-IR) at 25 °C or under TS.  $N=8-9$  per experimental group. **F** ROS levels brains of flies with depleted CIV (CIV-IR) in the presence (CIV-IR+ROT) or absence of rotenone (CIV-IR).  $N=8$  per experimental group. Data are shown as mean ± SEM. \*  $p < 0.05$ , \*\*\*  $p < 0.001$

rotenone and measuring mtROS (Fig. 4F). We did not observe a decrease in the presence of rotenone and therefore were able to discard ROS-RET as the mechanism of ROS generation. To confirm the results of our genetic model, we used the specific CIV inhibitor, cyanide, to acutely block CIV. This pharmacological model avoids the uncontrolled effects resulting from long-term adaptations to genetic depletion of CIV. Cyanide treatment mimicked the genetic model by inhibiting respiration by over 50% (Fig. S4E) and strongly increasing ROS levels. As seen with genetic inhibition of CIV, rotenone treatment did not decrease ROS levels (Fig. S4F), discarding ROS-RET as a source of ROS when CIV is blocked.

## Discussion

Here, we provide mechanistic evidence of how ROS-RET signalling is activated in response to TS and describe the metabolic response it initiates. We show that ROS-RET signalling is lost during ageing and demonstrate that reducing the ability to activate ROS-RET signalling decreases the capacity of flies to adapt to TS. Finally, we dissect the mechanisms which result in continuous production of mtROS in “old mitochondria,” demonstrating that this is caused by a limitation of electron exit.

Under TS, in young mitochondria ROS-RET is activated in response to increased electron entry through CI/CII and accessory dehydrogenases that are not part of the canonical ETC. This is similar to what has been reported in other scenarios where ROS-RET is triggered [38]. For example, ROS-RET is usually associated with increased oxidation of succinate by CII, like during ischemia reperfusion [6] or hypoxia within specialised cells of the carotid body [10]. However, ROS-RET is also activated in response to increased oxidation of fatty acids in cultured mouse cells [12] and isolated mitochondria when they are fed with sn-glycerol-3-phosphate [26] or products of choline oxidation [22]. Our metabolomics analysis indicates that these processes are potentially involved in activating ROS-RET production in the brain of young flies (Fig. 1).

Our data indicate that the production of ROS-RET initiates metabolic reprogramming consisting of rerouting glycolytic intermediates to the PPP (Fig. 2). This increases NADPH production providing cells

with both reductive and anabolic power. Accordingly, suppressing ROS-RET using rotenone completely depleted NADPH. Several observations support the idea that this stress response is conserved across evolution. Firstly, suppression of ROS signalling attenuates the long-term transcriptomic stress response in TS flies [41] and mice exposed to mitochondrial stress [9]. Secondly, a comparable “glycolysis-to-PPP-rerouting” response is observed in human cells in response to H<sub>2</sub>O<sub>2</sub> treatment [17]. Similarly, LPS triggers ROS-RET in macrophages [24], and this stimulates the rerouting of glycolytic intermediates to PPP to produce NADPH [4]. A mechanism which is also used by glioma stem cells to adapt to acidosis [47] and lung cancer cells to resist high levels of oxidative stress [2]. It is not completely clear mechanistically how this rerouting occurs, but inhibition of several glycolytic enzymes through oxidation of cysteine residues is the most likely explanation based on the evidence available. In accordance, oxidation of pyruvate kinase M2 in human cells [2] and GAPDH in yeast, worms, and human cells [31] has been described alongside interruption of glycolysis and boosting of PPP. However, an independent report showed that metabolic rerouting precedes changes in the activity of glycolytic enzymes in response to increases in H<sub>2</sub>O<sub>2</sub> [17]. We have not investigated the mechanisms by which ROS-RET activates NADPH synthesis in the fly brain in response to stress, a question which warrants further investigation. The metabolomic approach used in this study has certain limitations. Firstly, as we did not use metabolic flux analysis, we can only estimate the directionality of the metabolic changes observed, connecting them based on the previous literature. Secondly, due to the type of chromatography used -liquid- we are not detecting many metabolites that are potentially important in the context of ROS-RET but would require gas chromatography to be detected [50].

During ageing, there is an increase in the generation of mtROS [38] that will impact redox signalling. Here, we show that young mitochondria increase ROS production in response to specific stimuli such as TS and rotenone, while aged mitochondria continually produce high levels of ROS (Fig. 3). Specifically, we demonstrate that the capacity of fly brain mitochondria to produce a ROS-RET signal is progressively attenuated during ageing and that in old flies, CI cannot produce ROS in response to TS

or rotenone. Further depletion of ROS-RET signalling impacts stress adaptation, with old flies dying in response to TS in the presence of rotenone. We anticipate that interruption of ROS-RET signalling would also impact other processes that require mtROS, such as activation of macrophages [24], hypoxia signalling [10], and sleep regulation [16]. Although it would be tempting to suggest that some of these processes are altered during ageing due to disruptions in mitochondrial redox communication, further research, including experiments restoring ROS-RET activation in old individuals, is required.

Finally, we dissected the mechanisms that drive the overproduction of ROS in old mitochondria. We considered two possibilities which are supported by the literature, i.e., a decrease in electron entry or exit [32, 40]. Our results support that decreased electron exit is the main problem, as we observed an increase in mtROS in fly brains only when electron exit was blocked (Fig. 4). We propose that due to decreased electron flow during ageing, the ETC produces continuously high levels of ROS but is unable to produce a ROS-RET signal in response to specific stimuli such as TS. It is intriguing how and why, during ageing, CI is replaced by one or more generators inactive in younger individuals to be the main ROS generator in fly brain mitochondria. The most likely candidate to be activated during ageing is CIII, which has been shown to increase ROS when CIV is inhibited and has been described as the main generator of ROS in aged rat heart mitochondria [5, 27, 38]. However, different mitochondria may operate in different ways. For example, it has been reported that a mild knock-down of CI subunits in fly muscle increases mtROS and extends lifespan [29]. This study did not investigate neither the ROS source nor the capacity to generate ROS-RET after CI depletion. Furthermore, the authors did not investigate whether mutant flies were sensitised to stress. In the future, we will need to investigate mtROS production in different tissues and at different ages. This way, we will be able to confirm whether age-related changes occur similarly in all tissues and therefore the feasibility of implementing a general strategy to restore redox signalling or if tissue-specific interventions would be more appropriate. For example, in isolated mitochondria from the flight muscle, glycerol-3-phosphate dehydrogenase is a major generator of ROS, producing more ROS than CIII [25]. Further, it is possible that CIII's role as a

ROS generator becomes even more important during fly ageing when glycolysis is dysregulated [21]. Therefore, we may need to target different ROS generators in different tissues, although this would be a complicated route it may be the only way to generate redox interventions that impact human lifespan.

**Author contribution** CG performed ROS measurements, lifespan experiments and oxygraph analysis. RS assisted with lifespan and oxygraph experiments and edited the manuscript. AEHY performed oxygraph analysis. RVS, SHYL and LMM generated the transcriptomics data. AHU, ODKM and TZ performed the metabolomic experiments. FS prepared samples for transcriptomics and metabolomics analyses. AS and FS designed and supervised the project, analysed data, assembled the figures and wrote the first version of the manuscript. All authors contributed to analyse and discuss the results and revised the manuscript.

**Funding** This research was supported by a BBSRC grant (BB/R008167/2) and a Wellcome Senior Research Fellowship (212241/A/18/Z) to AS, an MRC DTP studentship to C.G., and a Henry Wellcome Postdoctoral Fellowship to RS (204715/Z/16/Z). RVS, SHYL and LMM are funded by the UK Medical Research Council, intramural project MC\_UU\_00025/3 (RG94521). AHU, ODKM and TZ were funded by a Cancer Research UK Career Development Fellowship (C53309/A19702).

#### Declarations

**Conflict of interest** The authors declare no competing interests.

**Open Access** This article is licensed under a Creative Commons Attribution 4.0 International License, which permits use, sharing, adaptation, distribution and reproduction in any medium or format, as long as you give appropriate credit to the original author(s) and the source, provide a link to the Creative Commons licence, and indicate if changes were made. The images or other third party material in this article are included in the article's Creative Commons licence, unless indicated otherwise in a credit line to the material. If material is not included in the article's Creative Commons licence and your intended use is not permitted by statutory regulation or exceeds the permitted use, you will need to obtain permission directly from the copyright holder. To view a copy of this licence, visit <http://creativecommons.org/licenses/by/4.0/>.

#### References

1. Albrecht SC, Barata AG, Grosshans J, Teleman AA, Dick TP. In vivo mapping of hydrogen peroxide and oxidized glutathione reveals chemical and regional specificity of redox homeostasis. *Cell Metab.* 2011;14(6):819–29.
2. Anastasiou D, Pouligiannis G, Asara JM, Boxer MB, Jiang JK, Shen M, Bellinger G, Sasaki AT, Locasale JW,

- Auld DS, Thomas CJ, Vander Heiden MG, Cantley LC. Inhibition of pyruvate kinase M2 by reactive oxygen species contributes to cellular antioxidant responses. *Science*. 2011;334(6060):1278–83.
3. Arias-Mayenco I, Gonzalez-Rodriguez P, Torres-Torrel H, Gao L, Fernandez-Aguera MC, Bonilla-Henao V, Ortega-Saenz P, Lopez-Barneo J. Acute O<sub>2</sub> sensing: role of coenzyme QH<sub>2</sub>/Q ratio and mitochondrial ROS compartmentalization. *Cell Metab*. 2018;28(1):145–158 e144.
  4. Baardman J, Verberk SGS, Prange KHM, van Weeghel M, van der Velden S, Ryan DG, Wust RCI, Neele AE, Speijer D, Denis SW, Witte ME, Houtkooper RH, O'Neill AL, Knatko EV, Dinkova-Kostova AT, Lutgens E, de Winther MPJ, Van den Bossche J. A defective pentose phosphate pathway reduces inflammatory macrophage responses during hypercholesterolemia. *Cell Rep*. 2018;25(8):2044–2052 e2045.
  5. Chen Q, Vazquez EJ, Moghaddas S, Hoppel CL, Lesnfsky EJ. Production of reactive oxygen species by mitochondria: central role of complex III. *J Biol Chem*. 2003;278(38):36027–31.
  6. Chouchani ET, Pell VR, Gaude E, Aksentijevic D, Sundier SY, Robb EL, Logan A, Nadochiy SM, Ord EN, Smith AC, Eyassu F, Shirley R, Hu CH, Dare AJ, James AM, Rogatti S, Hartley RC, Eaton S, Costa AS, Brookes PS, Davidson SM, Duchon MR, Saeb-Parsy K, Shattock MJ, Robinson AJ, Work LM, Frezza C, Krieg T, Murphy MP. Ischaemic accumulation of succinate controls reperfusion injury through mitochondrial ROS. *Nature*. 2014;515(7527):431–5.
  7. Cocheme HM, Quin C, McQuaker SJ, Cabreiro F, Logan A, Prime TA, Abakumova I, Patel JV, Fearnley IM, James AM, Porteous CM, Smith RA, Saeed S, Carre JE, Singer M, Gems D, Hartley RC, Partridge L, Murphy MP. Measurement of H<sub>2</sub>O<sub>2</sub> within living *Drosophila* during aging using a ratiometric mass spectrometry probe targeted to the mitochondrial matrix. *Cell Metab*. 2011;13(3):340–50.
  8. Correia-Melo C, Marques FD, Anderson R, Hewitt G, Hewitt R, Cole J, Carroll BM, Miwa S, Birch J, Merz A, Rushton MD, Charles M, Jurk D, Tait SW, Czapiewski R, Greaves L, Nelson G, Bohlooly YM, Rodriguez-Cuenca S, Vidal-Puig A, Mann D, Saretzki G, Quarato G, Green DR, Adams PD, von Zglinicki T, Korolchuk VI, Passos JF. Mitochondria are required for pro-ageing features of the senescent phenotype. *EMBO J*. 2016;35(7):724–42.
  9. Dogan SA, Cerutti R, Beninca C, Brea-Calvo G, Jacobs HT, Zeviani M, Szibor M, Viscomi C. Perturbed redox signaling exacerbates a mitochondrial myopathy. *Cell Metab*. 2018;28(5):764–775 e765.
  10. Fernandez-Aguera MC, Gao L, Gonzalez-Rodriguez P, Pintado CO, Arias-Mayenco I, Garcia-Flores P, Garcia-Perganeda A, Pascual A, Ortega-Saenz P, Lopez-Barneo J. Oxygen Sensing by arterial chemoreceptors depends on mitochondrial complex I signaling. *Cell Metab*. 2015;22(5):825–37.
  11. Goncalves RL, Rothschild DE, Quinlan CL, Scott GK, Benz CC, Brand MD. Sources of superoxide/H<sub>2</sub>O<sub>2</sub> during mitochondrial proline oxidation. *Redox Biol*. 2014;2:901–9.
  12. Guaras A, Perales-Clemente E, Calvo E, Acin-Perez R, Loureiro-Lopez M, Pujol C, Martinez-Carrasco I, Nunez E, Garcia-Marques F, Rodriguez-Hernandez MA, Cortes A, Diaz F, Perez-Martos A, Moraes CT, Fernandez-Silva P, Trifunovic A, Navas P, Vazquez J, Enriquez JA. The CoQH<sub>2</sub>/CoQ Ratio Serves as a Sensor of Respiratory Chain Efficiency. *Cell Rep*. 2016;15(1):197–209.
  13. Jacobson J, Lambert AJ, Portero-Otin M, Pamplona R, Magwere T, Miwa S, Driege Y, Brand MD, Partridge L. Biomarkers of aging in *Drosophila*. *Aging Cell*. 2010;9(4):466–77.
  14. Jevtov I, Zacharogianni M, van Oorschot MM, van Zadelhoff G, Aguilera-Gomez A, Vuillez I, Braakman I, Hafen E, Stocker H, Rabouille C. TORC2 mediates the heat stress response in *Drosophila* by promoting the formation of stress granules. *J Cell Sci*. 2015;128(14):2497–508.
  15. Jorgensen LB, Overgaard J, Hunter-Manseau F, Pichaud N. "Dramatic changes in mitochondrial substrate use at critically high temperatures: a comparative study using *Drosophila*." *J Exp Biol* 2021;224(Pt 6).
  16. Kempf A, Song SM, Talbot CB, Miesenbock G. A potassium channel beta-subunit couples mitochondrial electron transport to sleep. *Nature*. 2019;568(7751):230–4.
  17. Kuehne A, Emmert H, Soehle J, Winnefeld M, Fischer F, Wenck H, Gallinat S, Terstegen L, Lucius R, Hildebrand J, Zamboni N. Acute activation of oxidative pentose phosphate pathway as first-line response to oxidative stress in human skin cells. *Mol Cell*. 2015;59(3):359–71.
  18. Lopez J, Bessou M, Riley JS, Giampazolias E, Todt F, Rochegue T, Oberst A, Green DR, Edlich F, Ichim G, Tait SW. Mito-priming as a method to engineer Bcl-2 addiction. *Nat Commun*. 2016;7:10538.
  19. Lopez-Otin C, Blasco MA, Partridge L, Serrano M, Kroemer G. The hallmarks of aging. *Cell*. 2013;153(6):1194–217.
  20. Maddocks ODK, Athineos D, Cheung EC, Lee P, Zhang T, van den Broek NJF, Mackay GM, Labuschagne CF, Gay D, Kruiswijk F, Blagih J, Vincent DF, Campbell KJ, Ceteci F, Sansom OJ, Blyth K, Vousden KH. Modulating the therapeutic response of tumours to dietary serine and glycine starvation. *Nature*. 2017;544(7650):372–6.
  21. Ma Z, Wang H, Cai Y, Wang H, Niu K, Wu X, Ma H, Yang Y, Tong W, Liu F, Liu Z, Zhang Y, Liu R, Zhu ZJ, Liu N. "Epigenetic drift of H3K27me<sub>3</sub> in aging links glycolysis to healthy longevity in *Drosophila*." *Elife* 2018;7.
  22. Mailloux RJ, Young A, Chalker J, Gardiner D, O'Brien M, Slade L, Brosnan JT. Choline and dimethylglycine produce superoxide/hydrogen peroxide from the electron transport chain in liver mitochondria. *FEBS Lett*. 2016;590(23):4318–28.
  23. Martinez-Reyes I, Cardona LR, Kong H, Vasan K, McElroy GS, Werner M, Kihshen H, Reczek CR, Weinberg SE, Gao P, Steinert EM, Piseaux R, Budinger GRS, Chandel NS. Mitochondrial ubiquinol oxidation is necessary for tumour growth. *Nature*. 2020;585(7824):288–92.
  24. Mills EL, Kelly B, Logan A, Costa AS, Varma M, Bryant CE, Tourlomousis P, Dabritz JH, Gottlieb E, Latorre I, Corr SC, McManus G, Ryan D, Jacobs HT, Szibor M, Xavier RJ, Braun T, Frezza C, Murphy MP, O'Neill LA. Succinate dehydrogenase supports metabolic repurposing of mitochondria to drive inflammatory macrophages. *Cell*. 2016;167(2):457–470 e413.
  25. Miwa S, St-Pierre J, Partridge L, Brand MD. Superoxide and hydrogen peroxide production by *Drosophila* mitochondria. *Free Radic Biol Med*. 2003;35(8):938–48.

26. Miwa S, Riyahi K, Partridge L, Brand MD. Lack of correlation between mitochondrial reactive oxygen species production and life span in *Drosophila*. *Ann N Y Acad Sci*. 2004;1019:388–91.
27. Moghaddas S, Hoppel CL, Lesnfsky EJ. Aging defect at the QO site of complex III augments oxyradical production in rat heart interfibrillar mitochondria. *Arch Biochem Biophys*. 2003;414(1):59–66.
28. Murphy MP. How mitochondria produce reactive oxygen species. *Biochem J*. 2009;417(1):1–13.
29. Owusu-Ansah E, Song W, Perrimon N. Muscle mitochondrial hormesis promotes longevity via systemic repression of insulin signaling. *Cell*. 2013;155(3):699–712.
30. Perez-Arellano I, Carmona-Alvarez F, Martinez AI, Rodriguez-Diaz J, Cervera J. Pyrroline-5-carboxylate synthase and proline biosynthesis: from osmotolerance to rare metabolic disease. *Protein Sci*. 2010;19(3):372–82.
31. Ralser M, Wameling MM, Latkolik S, Jansen EE, Leh-rach H, Jakobs C. Metabolic reconfiguration precedes transcriptional regulation in the antioxidant response. *Nat Biotechnol*. 2009;27(7):604–5.
32. Ren JC, Rebrin I, Klichko V, Orr WC, Sohal RS. Cytochrome c oxidase loses catalytic activity and structural integrity during the aging process in *Drosophila melanogaster*. *Biochem Biophys Res Commun*. 2010;401(1):64–8.
33. Robb EL, Hall AR, Prime TA, Eaton S, Szibor M, Viscomi C, James AM, Murphy MP. Control of mitochondrial superoxide production by reverse electron transport at complex I. *J Biol Chem*. 2018;293(25):9869–79.
34. Sanz A, Stefanatos R, McIlroy G. Production of reactive oxygen species by the mitochondrial electron transport chain in *Drosophila melanogaster*. *J Bioenerg Biomembr*. 2010;42(2):135–42.
35. Sanz A, Fernandez-Ayala DJ, Stefanatos RK, Jacobs HT. Mitochondrial ROS production correlates with, but does not directly regulate lifespan in *Drosophila*. *Aging (Albany NY)*. 2010;2(4):200–23.
36. Scaraffia PY, Wells MA. Proline can be utilised as an energy substrate during flight of *Aedes aegypti* females. *J Insect Physiol*. 2003;49(6):591–601.
37. Schieber M, Chandel NS. ROS function in redox signaling and oxidative stress. *Curr Biol*. 2014;24(10):R453–462.
38. Scialo F, Sanz A. Coenzyme Q redox signalling and longevity. *Free Radic Biol Med*. 2021;164:187–205.
39. Scialo F, Sriram A, Stefanatos R, Sanz A. Practical recommendations for the use of the GeneSwitch Gal4 system to knock-down genes in *drosophila melanogaster*. *PLoS One*. 2016;11(8):e0161817.
40. Scialo F, Sriram A, Fernandez-Ayala D, Gubina N, Lohmus M, Nelson G, Logan A, Cooper HM, Navas P, Enriquez JA, Murphy MP, Sanz A. Mitochondrial ROS produced via reverse electron transport extend animal lifespan. *Cell Metab*. 2016;23(4):725–34.
41. Scialo F, Sriram A, Stefanatos R, Spriggs RV, Loh SHY, Martins LM, Sanz A. Mitochondrial complex I derived ROS regulate stress adaptation in *Drosophila melanogaster*. *Redox Biol*. 2020;32:101450.
42. Sorensen JG, Nielsen MM, Kruhoffer M, Justesen J, Loeschcke V. Full genome gene expression analysis of the heat stress response in *Drosophila melanogaster*. *Cell Stress Chaperones*. 2005;10(4):312–28.
43. Stefanatos R, Sanz A. The role of mitochondrial ROS in the aging brain. *FEBS Lett*. 2018;592(5):743–58.
44. Tormos KV, Anso E, Hamanaka RB, Eisenbart J, Joseph J, Kalyanaraman B, Chandel NS. Mitochondrial complex III ROS regulate adipocyte differentiation. *Cell Metab*. 2011;14(4):537–44.
45. Wallace DC. A mitochondrial paradigm of metabolic and degenerative diseases, aging, and cancer: a dawn for evolutionary medicine. *Annu Rev Genet*. 2005;39:359–407.
46. Xia J, Wishart DS. Using MetaboAnalyst 3.0 for Comprehensive Metabolomics Data Analysis. *Curr Protoc Bioinformatics*. 2016;55:14 10 11–14 10 91.
47. Xu X, Wang L, Zang Q, Li S, Li L, Wang Z, He J, Qiang B, Han W, Zhang R, Peng X, Abliz Z. Rewiring of purine metabolism in response to acidosis stress in glioma stem cells. *Cell Death Dis*. 2021;12(3):277.
48. Yang C, Ko B, Hensley CT, Jiang L, Wasti AT, Kim J, Sudderth J, Calvaruso MA, Lumata L, Mitsche M, Rutter J, Merritt ME, DeBerardinis RJ. Glutamine oxidation maintains the TCA cycle and cell survival during impaired mitochondrial pyruvate transport. *Mol Cell*. 2014;56(3):414–24.
49. Yang L, Garcia Canaveras JC, Chen Z, Wang L, Liang L, Jang C, Mayr JA, Zhang Z, Ghergurovich JM, Zhan L, Joshi S, Hu Z, McReynolds MR, Su X, White E, Morscher RJ, Rabinowitz JD. Serine catabolism feeds NADH when respiration is impaired. *Cell Metab*. 2020;31(4):809–821 e806.
50. Zeki OC, Eylem CC, Recber T, Kir S, Nemetlu E. Integration of GC-MS and LC-MS for untargeted metabolomics profiling. *J Pharm Biomed Anal*. 2020;190:113509.

**Publisher's note** Springer Nature remains neutral with regard to jurisdictional claims in published maps and institutional affiliations.